Concise CIO based precession-nutation formulations

Nicole Capitaine, Patrick Wallace

A&A 478, 277–284 (2008)
DOI: 10.1051/0004-6361:20078811

Astronomy & Astrophysics

Concise CIO based precession-nutation formulations⋆

N. Capitaine[1] and P. T. Wallace[2]

[1] Observatoire de Paris, SYRTE/UMR8630-CNRS, 61 avenue de l'Observatoire, 75014 Paris, France
e-mail: n.capitaine@obspm.fr
[2] Rutherford Appleton Laboratory, Harwell Science & Innovation Campus, Didcot, Oxfordshire OX11 0QX, UK
e-mail: P.T.Wallace@rl.ac.uk

Received 8 October 2007 / Accepted 7 November 2007

ABSTRACT

Context. The IAU 2000/2006 precession-nutation models have precision goals measured in microarcseconds. To reach this level of performance has required series containing terms at over 1300 frequencies and involving several thousand amplitude coefficients. There are many astronomical applications for which such precision is not required and the associated heavy computations are wasteful. This justifies developing smaller models that achieve adequate precision with greatly reduced computing costs.
Aims. We discuss strategies for developing simplified IAU 2000/2006 precession-nutation procedures that offer a range of compromises between accuracy and computing costs.
Methods. The chain of transformations linking celestial and terrestrial coordinates comprises frame bias, precession-nutation, Earth rotation and polar motion. We address the bias and precession-nutation (NPB) portion of the chain, linking the Geocentric Celestial Reference System (GCRS) with the Celestial Intermediate Reference System (CIRS), the latter based on the Celestial Intermediate Pole (CIP) and Celestial Intermediate Origin (CIO). Starting from direct series that deliver the CIP coordinates X, Y and (via the quantity $s + XY/2$) the CIO locator s, we look at the opportunities for simplification.
Results. The biggest reductions come from truncating the series, but some additional gains can be made in the areas of the matrix formulation, the expressions for the nutation arguments and by subsuming long period effects into the bias quantities. Three example models are demonstrated that approximate the IAU 2000/2006 CIP to accuracies of 1 mas, 16 mas and 0.4 arcsec throughout 1995–2050 but with computation costs reduced by 1, 2 and 3 orders of magnitude compared with the full model.

Key words. astrometry – ephemerides – reference systems – methods: numerical

1. Introduction

1.1. The IAU 2000/2006 models for Earth attitude

Many astronomical computations involve knowing the orientation of the Earth in space, i.e. the time-varying transformation between the terrestrial and celestial coordinate triads. The methods currently used to realize this transformation employ specific a priori models adopted by IAU resolutions in 2000 and 2006 together with time-dependent observed quantities provided by the International Earth rotation and Reference systems Service (IERS). The IAU 2000 and 2006 resolutions not only adopted greatly improved numerical models, but also a new procedural framework, with associated terminology for the pole, the Earth's angle of rotation, the longitude origins and the related reference systems.

The two triads correspond to the *International Terrestrial Reference System* (ITRS, IUGG Resolution 2, Perugia 2007) and the *Geocentric Celestial Reference System* (GCRS, IAU 2000 Resolution B1.3). The pole of the nominal rotation axis is the *Celestial Intermediate Pole* (CIP, IAU 2000 Resolution B1.7). The CIP moves within the ITRS because of *polar motion,* which is mainly quasi-periodic but essentially unpredictable, and within the GCRS because of *precession-nutation,* which includes both secular and periodic effects and is largely predictable.

The CIP's changing position in the GCRS has three components: (i) *frame bias,* a small fixed offset between the pole of the GCRS and the CIP at J2000.0; (ii) a *precession* model that describes the secular motion of the CIP; and (iii) a *nutation* model that describes the quasi-periodic part of the motion. Items (i) and (iii) are currently taken from the MHB2000 precession-nutation model (Mathews et al. 2002) that was adopted by IAU 2000 Resolution B1.6 to become IAU 2000A. Item (ii) is the P03 precession model of Capitaine et al. (2003b) that IAU 2006 Resolution B1 adopted as the replacement (from 2009) for the precession part of IAU 2000A; note that this requires small adjustments to the IAU 2000A nutation to restore consistency between the two components.

The terrestrial and celestial systems in which the CIP is the common pole are called the *Celestial Intermediate Reference System* (CIRS) and the *Terrestrial Intermediate Reference System* (TIRS). The diurnal rotation linking the two systems is expressed through a conventional linear transformation of UT1 called *Earth Rotation Angle* (ERA, IAU 2000 Resolution B1.8). ERA is used in conjunction with specific zero points of celestial and terrestrial longitude (i.e. right ascension), the *Celestial Intermediate Origin* (CIO, IAU 2000 Resolution B1.8 and IAU 2006 Resolution B2) and *Terrestrial Intermediate Origin* (TIO, idem as for CIO) respectively. The CIO is at present very close

⋆ Appendices A to G are only available in electronic form at http://www.aanda.org

to GCRS longitude zero and almost stationary in longitude. This contrasts with the former zero point of right ascension, the vernal equinox, which moves at over 50 arcsec per year in GCRS longitude. Similarly, the TIO is at present close to ITRS longitude zero and again is almost stationary in longitude. ERA can be thought of as the CIO based equivalent of *Greenwich Sidereal Time* (GST). The extremely simple form of the ERA(UT1) relation (Eq. (2)) is a reflection of the kinematically non-rotating nature of the CIO (Capitaine et al. 1986).

1.2. Earth orientation parameters

The a priori CIP and rotation models are supplemented by time-dependent observed quantities, published by the IERS, obtained from monitoring Earth attitude with respect to distant radio sources by very long baseline interferometry (VLBI). The quantities, known as *Earth orientation parameters* (EOPs), supplement the a priori models to achieve final accuracies that approach 100 μas. The IERS tabulations provide (i) *Universal Time,* UT1, the continuously changing angle representing the Earth's diurnal rotation; (ii) polar motion; and (iii) small adjustments to the CIP's GCRS X, Y coordinates as predicted by the a priori precession-nutation model, which is limited in the short term by free core nutation (FCN), which at present cannot be predicted, and in the long term by the uncertainties in the precession rates.

Few applications take account of the CIP dX, dY corrections, at present less than 1 mas, and some even neglect polar motion, which rarely exceeds 0.5 arcsec. However, in even the least demanding applications it is essential for the IERS UT1 observations, i.e. the published UT1−UTC or UT1−TAI values, to form the basis of the Earth rotation predictions.

1.3. The need for concise formulations

The IAU 2000A nutation model has extremely high precision goals, measured in microarcseconds. The terms that have to be evaluated in order to predict the GCRS coordinates of the CIP to the full precision of the model have been provided in Wallace & Capitaine (2006, denoted WC06 in the following) Table 1. The total number of coefficients varies somewhat depending on the adopted computational scheme, but in all cases is several thousand, with some below 1 μas.

Although in many applications computation time or program size are not limiting factors, the large size of the model is often at best an unnecessary overhead and at worst can exhaust the available resources. There is consequently a demand for precession-nutation implementations that offer different compromises between size and precision. This was understood at the time of the IAU 2000 resolutions, which in addition to the full IAU 2000A model also recognized a shortened model called IAU 2000B (published afterwards by McCarthy & Luzum 2003). IAU 2000B is more than an order of magnitude smaller than IAU 2000A but achieves 1 mas accuracy throughout 1995−2050. Moreover, the full models can be radically cut back before the rms performance compared with VLBI observations starts to degrade noticeably. For example Shirai & Fukushima (2001) retained only 194 terms (see their Fig. 1).

Examples of applications where concise precession-nutation formulations are used include:

- Satellite orbit predictions (see Vallado et al. 2006).
- Pulsar timing: the recent TEMPO2 analysis software (Edwards et al. 2006) uses the IAU 2000B model.

Table 1. Approximate expressions for the elements of the GCRS to CIRS rotation matrix.

$\mathbf{R}_{\rm NPB}$	Method B	Method C
(1, 1)	$1 - X^2/2$	1
(1, 2)	$-s - XY/2$	0
(1, 3)	$-X$	$-X$
(2, 1)	$s - XY/2$	0
(2, 2)	$1 - Y^2/2$	1
(2, 3)	$-Y - sX$	$-Y$
(3, 1)	X	X
(3, 2)	Y	Y
(3, 3)	$1 - (X^2 + Y^2)/2$	1

- The pointing of telescopes and radio dishes, limited by the mechanical imperfections in the mount and drives (rarely predictable to better than 1 or 2 arcsec) and also the ability to predict atmospheric refraction.
- Prediction of occultations, where each 1 mas of precession-nutation error moves the observer only 31 mm.

Such applications are of course distinct from those involving precise Earth rotation studies, accurate Doppler predictions for space telemetry, optical interferometry, VLBI, etc., where use of the full-accuracy models is necessary. However, in those cases where the celestial position of the pole must be known with full accuracy, and hence observed corrections to the model must be applied, a concise a priori model with matching corrections would deliver identical results with much improved computing efficiency. (Such a scheme would of course require an extension to the existing IERS services.) For example Petrov (2007) makes use of a very simplified a priori model that retains essentially the same precession-nutation terms as the concise model CPN_d presented later (Sect. 4.3).

1.4. The celestial to terrestrial transformation

Frame bias, precession-nutation, Earth rotation and polar motion form a chain of transformations connecting celestial coordinates (GCRS) to terrestrial coordinates (ITRS). In matrix form:

$$\mathbf{v}_{\rm ITRS} = \mathbf{R}_{\rm PM} \cdot \mathbf{R}_3(\theta) \cdot \mathbf{R}_{\rm NPB} \cdot \mathbf{v}_{\rm GCRS} \quad (1)$$

where:

- $\mathbf{v}_{\rm GCRS}$ and $\mathbf{v}_{\rm ITRS}$ are the same direction with respect to the two reference systems;
- the matrix $\mathbf{R}_{\rm NPB}$ represents the combined effects of frame bias and precession-nutation and defines the orientation of the CIP and a longitude origin;
- $\mathbf{R}_3(\theta)$ is Earth rotation, with θ either ERA or GST depending on whether $\mathbf{R}_{\rm NPB}$ is CIO based or equinox based, the result in either case being with respect to the TIRS; and
- the matrix $\mathbf{R}_{\rm PM}$ takes account of polar motion.

The rest of this paper is concerned with formulations for the matrix $\mathbf{R}_{\rm NPB}$ in its CIO based form, i.e. where θ is Earth Rotation Angle:

$$\theta(T_u) = 2\pi\,(0.7790572732640 + 1.00273781191135448\,T_u), \quad (2)$$

where T_u = (Julian UT1 date − 2451545.0) (Capitaine et al. 2000). Applications that instead must work with sidereal time and equinox based right ascension can simply use

$$\alpha_{\rm equinox} = \alpha_{\rm CIO} - \mathrm{EO} \quad (3)$$

and

$$\mathrm{GST} = \mathrm{ERA} - \mathrm{EO}, \quad (4)$$

where EO is the equation of the origins. See Sect. 2.2 of Capitaine & Wallace (2006, denoted CW06 in the following).

1.5. Starting point for concise formulations

Various methods of generating the matrix $\mathbf{R}_{\mathrm{NPB}}$ were provided in CW06. Any of these methods could in principle form the basis of a concise formulation, but that described in CW06 Sect. 2.1 is particularly suitable. It starts with the CIP's GCRS unit-vector coordinates X, Y and the CIO locator s, the latter being the difference between the GCRS and CIRS right ascensions of the intersection of the two equators.

Rigorous expressions for X, Y and s are given in CW06 Eqs. (33), (34), (56) and (57) and are functions of the bias and classical precession-nutation quantities. The three quantities can also be calculated as a function of time using series, in the case of X and Y directly and in the case of s through a series for $s + XY/2$. The series comprise polynomial, Fourier and Poisson terms, and by comparying the series and rigorous forms it is easy to see where these contributions come from.

The published series reproduce the theoretical values to microarcsecond accuracy over a century. For applications with reduced accuracy requirements, it is straightforward to limit the development to the appropriate level of approximation, eliminating smaller terms and thereby producing a concise formulation. Note that:

- Precession and nutation are combined and can be dealt with together.
- Each of the three series provides a quantity (namely X, Y or s) that contributes equally to the final accuracy, allowing the same cut-off criterion to be chosen in each case: there are no $\sin\epsilon$ factors to consider for example, as is the case for the classical precession and nutation angles in ecliptic longitude.
- The three quantities can be treated independently from the other opportunities for economies, namely the expressions for the fundamental arguments (see 3.5, later) and the matrix elements (3.4).

In this paper, we take the X, Y, $s+XY/2$ series method in its full-precision form and show how it can be reduced so as to achieve different trade-offs between accuracy and size/speed. Three examples are described, of 1 mas, 16 mas and 390 mas accuracy in the time span 1995−2050. The numerical coefficients of the three formulations are tabulated in Appendices E−G. Note that our goal is to establish a methodology for abridging the full-precision method and that our solutions involve neither fitting of amplitude coefficients nor harmonic analysis. Consequently they are not necessarily the most compact series possible for a given accuracy, but they are unlikely to be significantly worse and have the advantage that all the terms have a clear provenance.

1.6. Relationship to IAU 2000B

The work reported here has obvious parallels with the IAU 2000B precession-nutation model, but differs in a number of respects.

In the present paper we set out to deliver a single CIO based precession-nutation standard (namely IAU 2006/2000A), but offering choice in the compromise between accuracy and size/speed. The example implementations that we present in Sect. 4 have no independent canonical claim: each should be regarded simply as an approximate method of generating the same thing, namely the GCRS to CIRS transformation matrix $\mathbf{R}_{\mathrm{NPB}}$. IAU 2000B in contrast provides only a single cost/performance choice, namely 1 mas between 1995 and 2050, is classical in form and is IAU-approved.

Table 2. The concise models compared. See Sect. 4.

Model	Coeffs	Freqs	RMS	Worst	Speed
reference	4006	1309	–	–	1
IAU 2000B	354	77	0.28	0.99	7.6
CPN_b	229	90	0.28	0.99	15.3
CPN_c	45	18	5.4	16.2	138
CPN_d	6	2	160	380	890
		mas	mas		

For historical reasons there are two slightly different interpretations of IAU 2000B in use, one in the IAU Standards Of Fundamental Astronomy (SOFA) software collection (Wallace 1998) and one in McCarthy & Luzum (2003). The SOFA version isolates the nutation part of IAU 2000B and uses it along with the IAU 2000 frame bias and precession. The published version provides nutation angles which incorporate corrections for frame bias and precession, to be combined directly with the IAU 1976 precession. The SOFA version is, by a small margin, the more accurate of the two when compared with the SOFA implementation of IAU 2000A, achieving a maximum CIP error of 0.994 mas during 1995−2050, compared with 1.125 mas for the published version. (See Fig. A.1.)

As well as the question of which version to use, it is necessary to decide what, if any, adjustments are appropriate when using the IAU 2000B nutation in combination with other precession models, in particular IAU 2006. But as a pre-existing concise precession-nutation model, IAU 2000B provides a natural benchmark to the work described here, and for that reason is included in Table 2, comparing different formulations.

2. The full accuracy GCRS-to-CIRS matrix

In Sect. 1.5 we showed that the direct series for X, Y and $s+XY/2$ were a convenient starting point. These are of the form:

$$q = q_0 + q_1\,t + q_2\,t^2 + q_3\,t^3 + q_4\,t^4 + q_5\,t^5 + \sum_i \sum_{j=0}^{3} [(a_{\mathrm{s},j})_i t^j \sin(\mathrm{ARG}) + (a_{\mathrm{c},j})_i t^j \cos(\mathrm{ARG})] + \cdots \quad (5)$$

where q stands for X, Y and $s + XY/2$ respectively, ARG stands for various combinations of the *fundamental arguments* of the nutation theory, including both luni-solar and planetary terms, and t is the elapsed time in Julian centuries since J2000 (TDB, though in practice TT is used). The series are obtained by a semi-analytical procedure (see CW06, Sect. 3.1), using the software package GREGOIRE (Chapront 2003). The current series, based on P03 precession and MHB2000 nutation, comprise a total of nearly 6000 coefficients of which just over 4000 are non-zero. For details of where the series can be found, see CW06 p. 982, footnote 2. Expressions for the fundamental arguments are given in Capitaine et al. (2003a).

Once X, Y and s are known, the elements of the $\mathbf{R}_{\rm NPB}$ matrix can be rigorously formulated as follows (CW06 Eq. (25), for $\beta = s$):

$$\begin{aligned}
\mathbf{R}_{\rm NPB}(1,1) &= (1 - aX^2)\cos s + aXY \sin s,\\
\mathbf{R}_{\rm NPB}(1,2) &= -aXY \cos s - (1 - aY^2)\sin s,\\
\mathbf{R}_{\rm NPB}(1,3) &= -X \cos s + Y \sin s,\\
\mathbf{R}_{\rm NPB}(2,1) &= (1 - aX^2)\sin s - aXY \cos s,\\
\mathbf{R}_{\rm NPB}(2,2) &= -aXY \sin s + (1 - aY^2)\cos s,\\
\mathbf{R}_{\rm NPB}(2,3) &= -X \sin s - Y \cos s,\\
\mathbf{R}_{\rm NPB}(3,1) &= X,\\
\mathbf{R}_{\rm NPB}(3,2) &= Y,\\
\mathbf{R}_{\rm NPB}(3,3) &= 1 - a(X^2 + Y^2),
\end{aligned} \tag{6}$$

with:

$$a^{-1} = 1 + (1 - (X^2 + Y^2))^{1/2} \simeq 1 + Z. \tag{7}$$

The finished matrix expresses the transformation between GCRS and CIRS coordinates and is consistent with the IAU 2006/2000A precession-nutation model at microarcsecond level. This rigorous implementation would be the natural choice for all high-precision work.

3. Opportunities for approximation

Computing the full-accuracy matrix developed in the previous Section, using an efficiently-organized algorithm, involves several thousand amplitude coefficients and the sines and cosines of 1500 angles, plus hundreds of additional arithmetic operations. In some applications this is excessive, and we must seek opportunities for streamlining. The possibilities include simplified expressions for the matrix elements and fundamental arguments, and truncated series for X, Y and s.

3.1. X, Y series

The completeness of the X, Y series is the dominating factor controlling the size and accuracy of the final implementation. Each of these series is much larger than that for $s+XY/2$, and together they dwarf the contribution from the matrix formulation and the fundamental argument expressions.

There are several options for truncating the series, and which is the most efficient depends on how the final algorithm is to be organized. The "purest" approach is to eliminate vector terms below a given amplitude, where "amplitude" means the root-sum-square of the sine and cosine coefficients (i.e. the vector modulus) at the given frequency. However, for terms with a phase close to $n\pi/2$ – which in fact is the majority – this leaves considerable numbers of individual coefficients that are well below the cut-off and have been retained only because the other coefficient of the pair is well above. This means that, at least for the shorter series, the simple approach of applying the cut to individual coefficients works well, producing an efficient result. Figure 1 shows the effect of applying such a cut to the full X and Y series, the cut-off point ranging from 1 μas (retaining 1382 coefficients out of the original 4006) to 1 arcsec (retaining only 4 coefficients). The 1995−2050 worst-case CIP error ranges from just under 50 μas to just over 0.9 arcsec.

Over most of the range, the CIP error grows steadily with increasing cut-off, and a suitable cut-off for any desired CIP accuracy can be selected freely. However, the best choices are just before sudden increases, where the next coefficient to be cut would cause a disproportionate worsening. There are even cases where, for the 1995-2050 test interval, an increased cut-off, and consequent reduction in model size, happens to reduce the CIP error slightly.

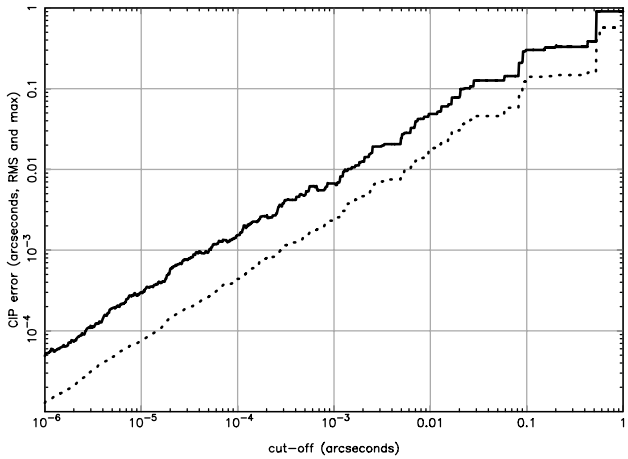

Fig. 1. The variation of CIP accuracy with differing cut-offs applied to the individual coefficients of the X, Y series. The horizontal axis is the cut-off in arcseconds. The vertical axis is the CIP accuracy, i.e. the distance between the CIP given by the truncated series and the CIP given by the full series. The heavy line shows for the indicated series truncation the maximum error during the interval 1995−2050; the dotted line is the rms error in the same interval.

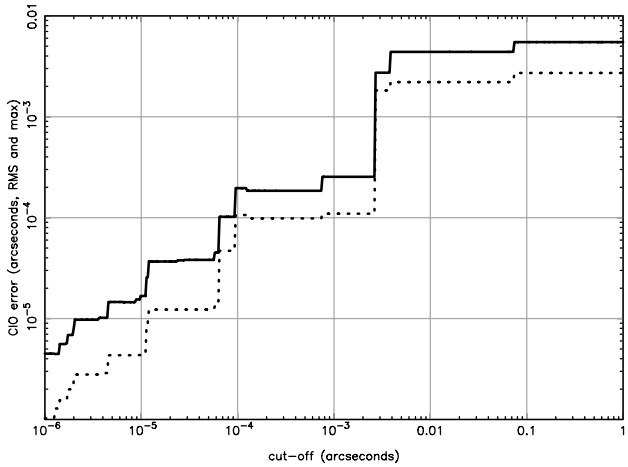

Fig. 2. The variation of s accuracy with differing cut-offs applied to the individual coefficients of the $s + XY/2$ series. The horizontal axis is the cut-off in arcseconds. The vertical axis is the error in the CIO locator s (using full-accuracy X and Y), compared with that predicted by the full series. The heavy line shows the maximum error during the interval 1995−2050; the dotted line is the rms error in the same interval.

The number of retained coefficients for a given cut-off C arcsec is roughly $3.6/10^{0.42 \log C}$, before eliminating any long-period terms (see Sect. 3.6).

Note that in certain applications in which the time derivative of the CIP motion is critical it is important to retain the frequencies that give rise to the largest amplitudes in the time derivatives of X and Y.

3.2. s + XY/2 series

Although the $s + XY/2$ series is much shorter than those for X and Y, there are potential savings if coefficients below a certain amplitude can be eliminated. Figure 2 shows the trade-off

between cut-off and accuracy in s and hence in the location of the CIO. It is clear that only a handful of coefficients is needed in order to achieve accuracies well under 1 mas.

As for the X, Y series but to a greater extent, reducing the cut-off level and consequently retaining additional coefficients causes different levels of improvement. Particularly favourable choices of cut-off are where 3, 7 and 17 coefficients are retained. The accuracies achieved by the 3- and 7-coefficient series are shown in Figs. F.3 and E.3 respectively.

It should be borne in mind that Fig. 2 uses full-accuracy X and Y values to remove the $XY/2$ component, and that given the circumstances under which a concise model for s is needed these will have themselves been calculated using approximate models. However, the accuracy requirements for X and Y are modest. Even after 1 century, X and Y will have reached only 2004 arcsec and 22 arcsec respectively, and so an error in each of 1 arcsec, for example, would cause an error in s of less than 5 mas, a negligible additional contribution. When the calculations for Fig. 2 were repeated using an X, Y model consisting of only four coefficients – a t term in X, a t^2 term in Y, and the Ω nutations in X and Y – the additional 1995−2050 error in s was under 2 mas, compared with the corresponding CIP error of nearly 1 arcsec.

For the most approximate formulations, it is acceptable to neglect s altogether, which leads to maximum errors of 22 mas during the test interval. The left-hand point in Fig. 2 shows that even the simplest approximation, namely $s = -XY/2$, is good to 6 mas.

3.3. The polynomial terms

The series used in Figs. 1 and 2 contain both polynomial terms and periodic (Fourier and Poisson) terms. The polynomial terms are few in number – only six coefficients for each of X, Y and $s + XY/2$, including constant terms – but dominate in the long term, and the choice of cut-off point is highly dependent on the time span which the concise model is aiming to support.

The X and Y polynomials are due essentially to precession and around J2000 are dominated by the t and t^2 terms respectively. Consequently, the more concise models omit terms from t^2 upwards in X and from t^3 upwards in Y (and perhaps the t term as well). In the case of $s + XY/2$, the coefficients fall away abruptly after t^3.

Figure B.1 demonstrates the effects of truncating the three polynomials at the natural places, namely t^2, t^3 and t^4 respectively. It can be seen that in each case the errors are not distributed symmetrically about J2000. This is merely a chance phenomenon, but we must expect the concise models to display similar asymmetries.

Because the polynomial terms are so few, the truncation level will have little effect on efficiency, and if long-term accuracy is important to the target application it would be reasonable to apply a less severe cut-off than that used for the periodic terms. However, the example concise models given later assume a strict 1995−2050 timespan and disregard the deteriorating performance outside this interval.

3.4. Matrix formulation

Five degrees of approximation of the matrix element expressions set out in Eqs. (6) were considered in WC06 Table 2; in the 21st century the errors introduced by the approximations range from 1 nanoarcsecond to 0.1 arcsec. Of the five formulations, two seem particularly suitable for our purposes, and these are reproduced as Methods B and C in Table 1 of the present paper.

Without trigonometric functions or square roots, Method B achieves a 21st-century precision of 8 μas (and better than 1 μas during the interval 1995−2050), well within the intrinsic accuracy of the precession-nutation model itself and therefore a usable basis for any shortened implementation.

Despite neglecting the CIO locator s completely, in the process removing the need to evaluate an $s + XY/2$ series, Method C achieves 25 mas precision throughout 1995−2050, which is more than adequate for many low-accuracy applications.

However, as the WC06 paper points out, simplifying the expressions for the matrix elements will not on its own achieve a significant reduction in the amount of computation: the bulk of any gains must come from the computation of X, Y and s.

3.5. Fundamental arguments

The fundamental arguments are a set of 14 angles, each an almost linear function of time. Five are Delaunay's nutation arguments, eight are planetary longitudes and the remaining one is general precession. These angles are used singly and in combination when evaluating the series for X, Y and $s + XY/2$.

The set of fundamental-argument expressions in Capitaine et al. (2003a), Eqs. (B.2) (luni-solar), Table B.1 (planetary) and Eq. (B.3) (precession) are suitable for use with the latest X, Y and $s + XY/2$ series and are close to those used in the IAU 2000A nutation model. Each angle is modeled as a polynomial in TDB (in practice TT is used, which has a negligible effect on the corresponding amplitudes of nutation). Each Delaunay variable has five coefficients, up to order t^4, while the remaining angles each require only two coefficients.

The opportunities for savings are not great, and occur mainly through a given argument not being needed rather than from reducing the order of polynomial. For the most concise and least accurate formulations, where only the Delaunay variables are required (and perhaps not all of those), it is enough to retain only the linear terms (Table C.1). For 1995−2050 this leads to errors of 32 μas (RMS) and 83 μas (worst case). For more accurate formulations, a possible compromise is to retain also the t^2 term, which during 1995−2050 achieves a worst case 0.042 μas and even over the four centuries 1800−2200 never contributes more than 2.7 μas.

3.6. Long period nutation

The IAU 2006/2000A X, Y series contain terms at 1309 frequencies, the periods ranging from 3.5 days to 93.3 millennia. In the short time span for which a concise version of the series is expected to operate, the terms of longer period will produce nearly fixed offsets in X and Y. When constructing IAU 2000B, McCarthy & Luzum (2003) subsumed these offsets into the frame bias, to boost efficiency, and we shall do the same. It is of course possible to go further and to represent the current portion of the very long period component as a polynomial: see Souchay et al. (2007).

Deciding where to place the cut-off period depends on the time span chosen and on the amplitudes of the terms. Given that the savings are likely to be modest, we can afford to be conservative and retain periodic terms below 1000 years period. Furthermore, by choosing J2000 as the date for computing the offsets, we need retain only the Fourier coefficients, of which there are 33 (Table D.1).

At J2000, this selection of very long period terms contributes offsets of −634.24 μas in X and +1421.45 μas in Y (cf. the McCarthy & Luzum empirically determined values, −629.9 μas and +1633.9 μas). When combined with the frame bias the final fixed terms are −17 251 μas in X and −5530 μas in Y. Note that these values can be used with any of the concise series, irrespective of accuracy goals: they amount to an adjusted frame bias for use whenever the nutation model neglects terms of greater than 1000 year period. Using the adjusted values will not necessarily reduce the peak errors – it is a matter of chance – but will in general improve the rms. For example in the example 42-coefficient NPB formulation (Table F.1), the 1995−2050 rms CIP error improved from 5701 μas to 5417 μas, while the peak CIP error happened to worsen slightly, from 16 046 μas to 16 153 μas. For any given formulation and time interval it would, of course, be possible to fit optimized constant terms, but in the concise formulations of the present paper we have retained the theoretical values.

4. Example concise formulations

There is, of course, no one concise NPB formulation that will suit all, or even a wide range of, applications. Nor is there, given a specific accuracy goal, a single optimum formulation. However, the results reported in Sect. 3 provide a basis for developing a concise formulation for a given application, containing a balanced set of optimizations and delivering a suitable compromise between computational costs and accuracy. We describe three such formulations that span a wide range of accuracy goals.

The performance of the three formulations is summarized in Table 2, with respect to (i) the full accuracy X, Y, s and (ii) IAU 2000B. Notes:

- The coefficient numbers are for non-zero polynomial and amplitude coefficients only and omit fundamental argument expressions (and, in the case of the equinox based IAU 2000B model, the additional 15 coefficients needed for the IAU 1976 precession, the precession-rate corrections, and the obliquity).
- The IAU 2000B comparison is with respect to the IAU 2000A model, equinox based; the others are with respect to IAU 2006/2000A, CIO based.
- The IAU 2000B and reference implementations are from the IAU SOFA software.
- The speeds (relative to the full implementation) are a rough guide to what can be expected without compiler optimization and using straightforward implementations. Manual optimizations, such as minimizing the computation of trigonometrical functions by using angle addition formulas, may produce additional speed gains.

In all the concise formulations we have rounded the coefficient values to 1 μas. This is done chiefly for convenience: computing costs are essentially unaffected. The quoted values can be truncated without materially affecting the results, should this be beneficial.

The series for three example formulations, designated CPN_b, CPN_c and CPN_d, are set out in Tables E.1−E.4, F.1, and G.1. The successive tabulations are arranged in different ways chosen in order to make the presentation as clear as possible in each case.

4.1. Concise model CPN_b: comparable with IAU 2000B

Similar performance to IAU 2000B can be achieved by a cut-off at about 50 μas, which leaves an X, Y model of 220 coefficients. A 7-coefficient series for $s+XY/2$, corresponding to a cut-off at about 60 μas, is enough to keep the overall accuracy within the 1 mas goal, making a total of 227 coefficients. The series includes terms at 90 frequencies, midway between the 106 used by the IAU 1980 nutation series and the 77 of the (SOFA) IAU 2000B series. At this level, there is little to be gained by truncating the fundamental-argument polynomials, and the tests reported here used the full expressions given in Capitaine et al. (2003a). The series is set out in Tables E.1−E.4, and the resulting X, Y and s can be used with the Table 1 Method B formulation for $\mathbf{R}_{\mathrm{NPB}}$. The 1800−2200 accuracy of the final algorithm is plotted in Fig. 3; performance is well maintained before and, to a lesser extent, after the 1995−2050 test interval. Figures E.1−E.3 show the error contributions from X, Y and s separately, and reveal that the worsening performance in the 22nd century comes mainly from the s component. The effect could be reduced by reinstating the t^4 and t^5 terms that the 7-coefficient $s+XY/2$ model omits; however, there would be a negligible improvement in the 1995−2050 interval for which the model is designed.

The level of precision that this model achieves is just above the natural "noise floor" set by FCN.

The 50 μas numerical cut-off of the X, Y portion of the CPN_b model corresponds to analytical developments of the X, Y quantities at the:

- 4th order in the precession quantity ψ_A,
- 2nd order in the nutation quantities $\Delta\psi$, $\Delta\epsilon$,
- 1st order in the precession quantities $(\omega_A - \epsilon_0)$, $(\epsilon_A - \epsilon_0)$ and χ_A,
- 1st order in the frame bias quantities ξ_0, η_0 and $\mathrm{d}\alpha_0$, and
- 3rd order in the cross terms between the precession quantity ψ_A and nutation (i.e. there are terms of the form $\psi_A^2\times$nutation),

as follows:

$$\begin{aligned} X \;=\; & \xi_0 + \psi_A \sin\epsilon_0 - (\psi_A^3/6)\sin\epsilon_0 + \psi_A(\omega_A - \epsilon_0)\cos\epsilon_0 \\ & + \Delta\psi \sin\epsilon_0 + \Delta\psi\Delta\epsilon \cos\epsilon_0 \\ & + (\psi_A \cos\epsilon_0 - \chi_A)\,\Delta\epsilon + (\epsilon_A - \epsilon_0)\,\Delta\psi\cos\epsilon_0 \\ & - (\psi_A^2/2)\,\Delta\psi\sin\epsilon_0 \end{aligned} \tag{8}$$

$$\begin{aligned} Y \;=\; & \eta_0 + (\omega_A - \epsilon_0) - (\psi_A^2/2)\sin\epsilon_0\cos\epsilon_0 \\ & + (\psi_A^4/24)\sin\epsilon_0\cos\epsilon_0 + d\alpha_0\,\psi_A\sin\epsilon_0 \\ & + \Delta\epsilon - (\Delta\psi^2/2)\sin\epsilon_0\cos\epsilon_0 \\ & - (\psi_A\cos\epsilon_0 - \chi_A)\,\Delta\psi\sin\epsilon_0 \\ & - (\psi_A^2/2)\cos\epsilon_0^2\,\Delta\epsilon. \end{aligned} \tag{9}$$

The above expressions contain

- polynomial terms of t (1st line in X and 1st two lines in Y) up to the 3rd degree for X and 4th degree for Y, which are due to bias and precession and
- periodic terms.

The periodic terms (from the 2nd and 3rd lines in X and Y, respectively) are composed of

- the classical nutation terms (i.e. Fourier terms with a few first degree Poisson terms) and cross nutation terms and
- first and second degree Poisson terms in sine and cosine due to cross terms between precession and nutation.

Note that the first degree Poisson terms (3rd line in X and 4th line in Y) with amplitudes larger than 50 μas correspond to nutation

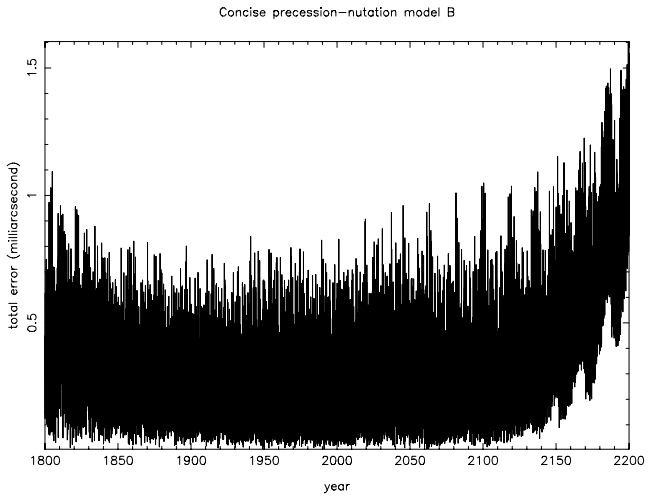

Fig. 3. The 400-year performance of the concise formulation described in Sect. 4.1 and designated CPN$_b$: see Tables E.1−E.4. The quantity plotted is the total rotational error of the CPN$_b$ NPB matrix, compared with that from the full series.

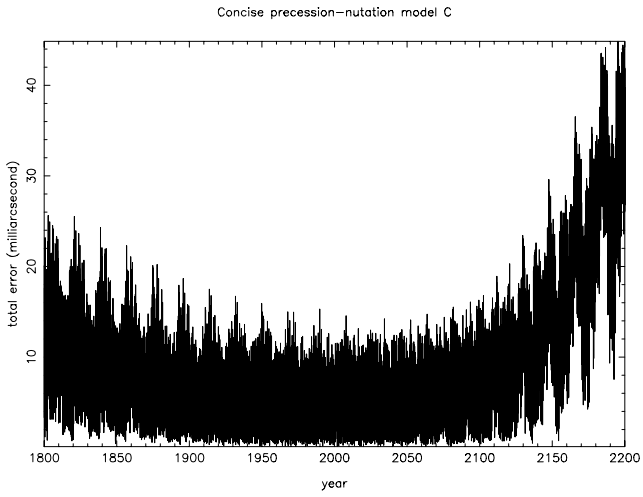

Fig. 4. The 400-year performance of the very concise formulation described in Sect. 4.2, set out in Table F.1 and designated CPN$_c$. Fundamental argument expressions from Table C.1 were used. The quantity plotted is the total rotational error of the CPN$_c$ NPB matrix, compared with that from the full series.

terms with amplitudes larger than 2 mas, while the second degree Poisson terms (4th line in X and 5th line in Y) larger than 50 μas correspond to nutation terms with amplitudes larger than 0.″4 and 0.″2 in longitude and obliquity, respectively. Only the cross nutation term corresponding to the 18.6-yr nutation is larger than the 50 μas limit.

The 60 μas numerical cut-off of the $s + XY/2$ portion of the CPN$_b$ model corresponds to analytical development of the $s + XY/2$ quantity at the:

- 1st order in the largest polynomial development coefficients $(X_i,Y_i)_{i=0,2}$ of X and Y, and
- 1st order in the coefficients a_i, b_i of the sine and cosine Fourier terms of arguments $(\omega_i t - \phi_i)$ in X and Y, respectively,

as follows:

$$\begin{aligned} s + XY/2 \;=\; & [X_1 Y_0 \;+ (1/2)\Sigma_i(a_i b_i \omega_i)]\; t + (1/3)\; X_1 Y_2 t^3 \\ & + (a_i b_i/4) \sin 2(\omega_i t - \phi_i) + (b_i/\omega_i) X_1 \sin(\omega_i t - \phi_i) \\ & + Y_2 t^2\; a_i \sin(\omega_i t - \phi_i). \end{aligned} \qquad (10)$$

This expression contains a polynomial of t up to the 3rd degree and periodic terms. The Fourier terms are at the nutation frequencies and at twice the frequency of nutation terms with sufficient amplitudes (note that only the 18.6-yr nutation has an amplitude sufficient to yield such a term with an amplitude larger than 60 μas). The second degree Poisson terms larger than 60 μas correspond to the nutation terms with amplitudes larger than 0.″6 (i.e. the 18.6-yr nutation only).

It should be noted that the CPN$_b$ series and the above simplified theoretical expressions are not an exact match because of the way in which the truncation has been done (see Sect. 3.1), namely coefficient by coefficient in the series rather than term by term in the theoretical expressions.

4.2. Concise model CPN$_c$: 16 mas accuracy

A cut-off at 2.5 mas removes from the X, Y series all coefficients of t^2 and above, leaving 42 coefficients. Throughout 1995−2050, this CIP model delivers worst-case accuracy of 16 mas, well above the level at which FCN needs to be taken into account and, relevant to applications like telescope pointing, well below the level set by atmospheric refraction predictions. This is considerably better than the still widely used (and much larger) IAU 1976/1980 precession-nutation model, though of course in the latter case the source of the inaccuracy is the incorrect precession rates rather than the nutation model. A 3-coefficient series for $s + XY/2$ (corresponding to a 2 mas cut-off) is a good match, and using the fundamental argument expressions from Table C.1 makes a total of 55 coefficients. The series is set out in Table F.1, and the resulting X, Y and s can be used with the Table 1 Method B formulation for $\mathbf{R}_{\rm NPB}$. The 1800−2200 accuracy of the final algorithm is plotted in Fig. 4, with the separate X, Y and s contributions in Figs. F.1−F.3. In this case the divergence after the 1995−2050 interval happens to come from the Y polynomial and could be remedied by reinstating the t^3 and t^4 terms.

At this level of approximation, Eqs. (8)−(10) can be reduced to:

$$\begin{aligned} X = {} & \xi_0 + \psi_A \sin\epsilon_0 - (\psi_A^3/6) \sin\epsilon_0 + \;\Delta\psi \sin\epsilon_0 \\ & + \psi_A \Delta\epsilon \cos\epsilon_0 + (\epsilon_A - \epsilon_0)\; \Delta\psi \cos\epsilon_0 \end{aligned}$$

$$\begin{aligned} Y = {} & \eta_0 \;+ (\omega_A - \epsilon_0) - (\psi_A^2/2) \sin\epsilon_0 \cos\epsilon_0 \\ & + \Delta\epsilon - \psi_A \Delta\psi \sin\epsilon_0 \cos\epsilon_0 \end{aligned}$$

$$\begin{aligned} s + XY/2 = {} & (1/2)\; \Sigma_i(a_i b_i \omega_i)\; t + (1/3)\; X_1 Y_2 t^3 \\ & + (b_i/\omega_i)\; X_1 \sin(\omega_i t - \phi_i). \end{aligned} \qquad (11)$$

One change with respect to the previous case is that the polynomial of t in Y is now reduced to the second degree. There are no longer any 2nd degree Poisson terms in any of the expressions for X, Y or $s + XY/2$, nor the Fourier term with twice the principal nutation frequency in $s + XY/2$, nor the cross terms between bias and precession in Y. Due to the ∼50× larger cut-off than for the previous model, the 1st order Poisson terms in X and Y result here from nutation terms with amplitudes larger than 0.″1 (i.e. only two terms).

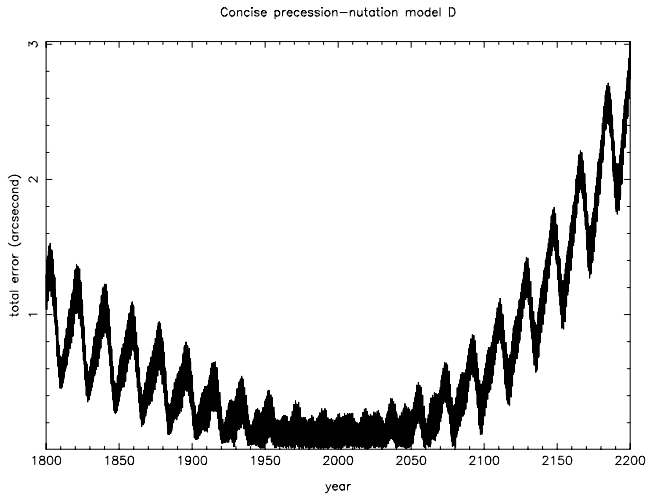

Fig. 5. The 400-year performance of the extremely concise formulation described in Sect. 4.3. The quantity plotted is the total rotational error of the CPN_d NPB matrix, compared with that from the full series.

4.3. CPN_d: an extremely concise formulation

For many applications, even lower accuracy is acceptable in order to achieve maximum savings in model complexity and computing overhead. For example, in pointing control systems for small telescopes (let alone the prediction of naked-eye phenomena) there is very little to be gained from going below 1 arcsec performance. Quite apart from the accuracy needs themselves, it is unlikely the such applications addressed by such a model would bother to take into account polar motion, which on its own introduces a contribution at the level of 0.5 arcsec.

Between 1995 and 2050, 1 arcsec worst case accuracy could be achieved by using an X, Y model of only four coefficients, namely a t term in X, a t^2 term in Y, and the main 18.6 y nutation term. However, the considerable additional accuracy available if the next largest nutation term (0.5 y) is included, compared with the limited improvements conferred by the next several terms, make a six coefficient model (Table G.1 and Fig. 5) attractive. This achieves a worst case accuracy of 0.39 arcsec throughout 1995−2050. At this level, the CIO locator s can be omitted altogether and the elements of the GCRS-to-CIRS matrix $\mathbf{R}_{\rm NPB}$ computed using Table 1 Method C. The arguments Ω and $A \equiv 2F - 2D + 2\Omega$ each require only two coefficients. In radians:

$$\Omega \approx 2.182439196616 - 33.7570459536t$$
$$A \approx -2.776244621014 + 1256.6639307381t \qquad (12)$$

(n.b. For neatness, the coefficients can, for this application, be rounded to three decimal places without significant loss of accuracy, though this is unlikely to affect computing costs.) We note that a total of 12 coefficients, which includes the two needed for the calculation of Earth Rotation Angle, Eq. (2), is enough to predict Earth orientation to better than 1 arcsec throughout the 1995−2050 test interval, or better than 0.4 arcsec if polar motion were to be taken into account. Even over 400 years (Fig. 5) the errors peak at only 3 arcsec. The individual X, Y and s contributions plotted in Figs. G.1−G.3 show that the truncation of the X polynomial is the post-2050 limitation in this case and that reinstating the t^2 and t^3 terms could be considered.

At this level of approximation, Eqs. (8)−(10) can be reduced to:

$$X = \psi_A \sin\epsilon_0 + \Delta\psi \sin\epsilon_0$$
$$Y = -(1/2)\sin\epsilon_0 \cos\epsilon_0 \psi_A^2 + \Delta\epsilon$$
$$s = 0. \qquad (13)$$

With such reduced accuracy requirements, the polynomial of t in X or Y, which comes here from the precession in longitude alone, includes only a 1st degree t term in X and a 2nd degree t term in Y, and the periodic part is reduced to the two largest nutation terms, the first from the nutation in longitude alone and the second from the nutation in obliquity alone.

5. Summary

In this paper we have discussed strategies for developing simplified IAU 2000/2006 precession-nutation procedures, using the CIO based paradigm, that offer a range of compromises between accuracy and computing costs. We have shown that the biggest reductions come from truncating the series for X, Y and $s+XY/2$, but that some additional gains can be made in the areas of the matrix formulation, the expressions for the nutation arguments and by subsuming long period effects into the bias quantities. We have shown how to calculate efficiently the bias-precession-nutation matrix for a given accuracy goal. The three example formulations presented span a three-order-of-magnitude range of size, speed and accuracy and can be used in a wide variety of applications where the utmost accuracy is not required.

Appendices E−G contain the numerical tables that define the three example models discussed.

Acknowledgements. We are grateful to the anonymous referee for helpful suggestions.

References

Capitaine, N., & Wallace, P. T. 2006, A&A, 450, 855 (CW06)
Capitaine, N., Guinot, B., & Souchay, J. 1986, Celest. Mech., 39, 283
Capitaine, N., Guinot, B., & McCarthy, D. D. 2000, A&A, 355, 398
Capitaine, N., Chapront, J., Lambert, S., & Wallace, P. T. 2003a, A&A, 400, 1145
Capitaine, N., Wallace, P. T., & Chapront, J. 2003b, A&A, 412, 567
Chapront, J. 2003, Notice, Paris Observatory (January 2003)
Edwards, R. T., Hobbs, G. B., & Manchester, R. N. 2006, MNRAS, 369, 655
McCarthy, D. D., & Luzum, B. J. 2003, Celest. Mech. Dyn. Astron., 85, 37
Mathews, P. M., Herring, T. A., & Buffett, B. A. 2002, J. Geophys. Res., 107, B4
Petrov, L. 2007, A&A, 467, 359
Shirai, T., & Fukushima, T. 2001, AJ, 121, 3270
Souchay, J., Lambert, S. J., & Le Poncin-Lafitte, C. 2007, A&A, 472, 681
Vallado, D. A., Seago, J. H., & Seidelmann, P. K. 2006, 16th AIAA/AAS Astrodynamics Specialist Conference, Tampa, FL, Jan. 22−26, 2006, AAS 06-134
Wallace, P. T. 1998, Highlights of Astronomy Vol. 11A, ed. J. Andersen (Kluwer Academic Publishers), 11, 191
Wallace, P. T., & Capitaine, N. 2006, A&A, 459, 981 (WC06)

Online Material

Appendix A: IAU 2000B series

For comparison with concise formulation CPN_b (Fig. 3), Fig. A.1 shows the performance of the IAU 2000B abridged nutation between 1800 and 2200, both as implemented by SOFA and as published. The comparisons are with respect to the SOFA implementation of IAU 2000A, which treats the frame bias and precession-rate corrections separately rather than combining them with the nutation.

It should be borne in mind that the 400-year interval shown in the graphs extends well outside the 1995−2050 interval for which the IAU 2000B series was designed. CPN_b and the two IAU 2000B versions all achieve similar performance in this interval. The superior performance of CPN_b outside the interval is mainly due to the inclusion of a handful of planetary terms, the periodic part of IAU 2000B being purely luni-solar.

n.b. The plots do not reproduce fully the peak errors, which occur during very narrow time ranges.

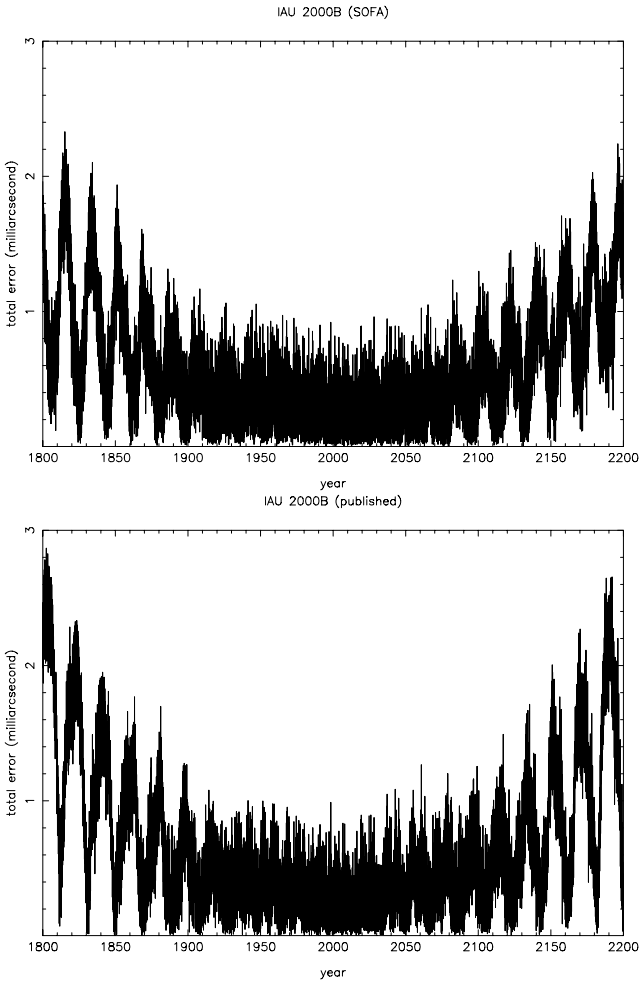

Fig. A.1. The 400-year performance of the IAU 2000B series. The vertical axis is the total rotational difference between the IAU 2000A and IAU 2000B equinox based NPB matrices. The upper graph is the series as implemented by SOFA; the lower graph is the series as subsequently published.

Appendix B: Polynomial truncation

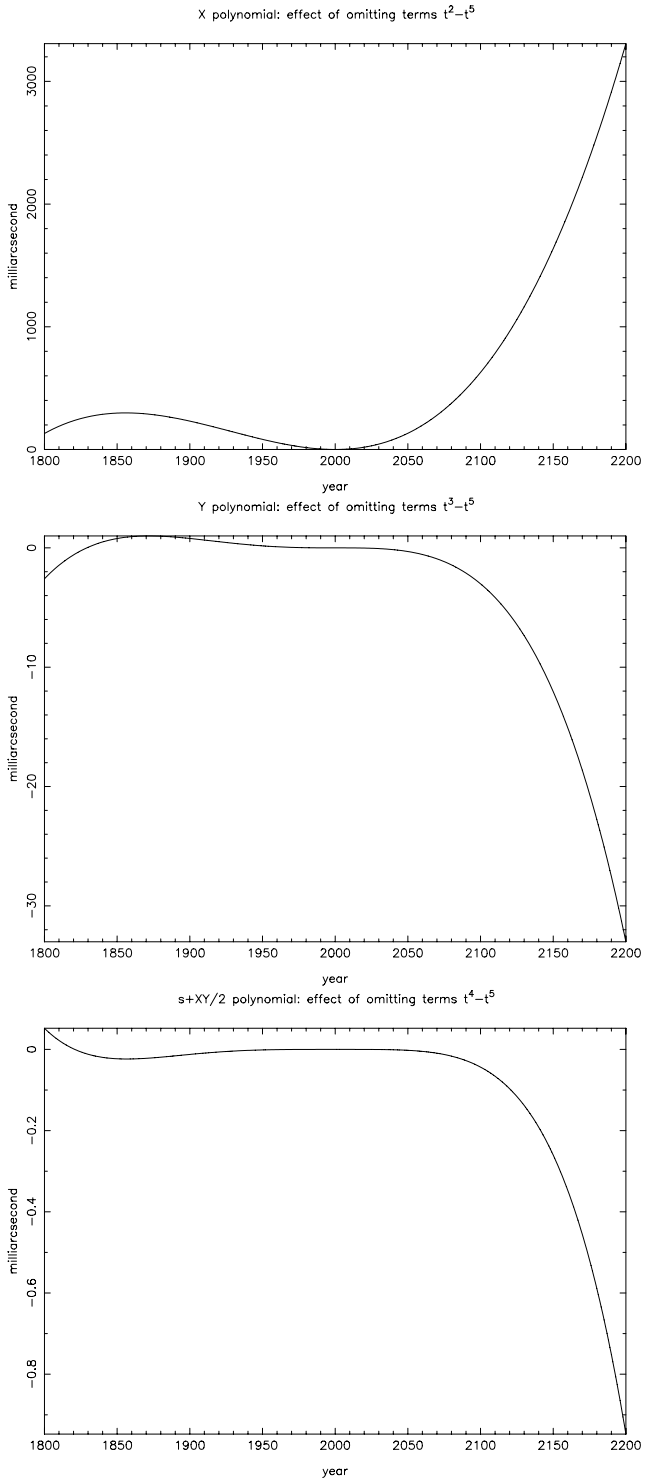

Fig. B.1. The inaccuracies in X (*upper*), Y (*middle*) and $s+XY/2$ (*lower*) that results from truncating the polynomials after the t, t^2 and t^3 terms respectively.

Appendix C: Fundamental arguments

Table C.1 Shows approximate expressions for the Delaunay variables as linear functions of time t, taken from the series given in Capitaine et al. (2003a), Table B.1. Neglecting terms of t^2 and above in this way leads to errors in the nutation predictions of less than 0.1 mas during the 1995−2050 test interval.

Table C.1. Linear approximations for the Delaunay variables.

Angle		t
l	2.3555557435	+8328.6914257191
l'	6.2400601269	+628.3019551714
F	1.6279050815	+8433.4661569164
D	5.1984665887	+7771.3771455937
Ω	2.1824391966	−33.7570459536
	radian	radian Jcy^{-1}

Appendix D: Long period nutation

Table D.1 shows nutation terms (Fourier) of period longer than 1 Julian millennium. The net value of these terms at J2000, namely −634.24 μas in X and +1421.45 μas in Y (Sect. 3.6), can be used computationally as ad hoc adjustments to the frame bias.

Table D.1. Very long-period nutation terms. The first five fundamental-argument multipliers are for the Delaunay variables, the next seven the planetary longitudes ($L_{\rm Me}$ not being required) and the final one general precession.

Period (years)	Term		Amplitude (μas)	l	l'	F	D	Ω	$L_{\rm Ve}$	$L_{\rm E}$	$L_{\rm Ma}$	$L_{\rm Ju}$	$L_{\rm Sa}$	$L_{\rm Ur}$	$L_{\rm Ne}$	p_A
20936.834154	X	cos	−79.08	0	1	−1	1	−1	0	0	0	0	0	0	0	0
11321.399513	X	cos	−1.71	0	0	0	0	0	0	8	−16	4	5	0	0	2
14949.752627	X	cos	−4.65	0	0	0	0	0	0	8	−16	4	5	0	0	−2
2024.979608	X	cos	−0.28	0	0	0	0	0	0	4	−8	1	5	0	0	−2
3186.025428	X	cos	+0.20	0	0	0	0	0	0	0	0	0	0	1	−2	−2
1540.710562	X	cos	+0.24	0	0	0	0	0	0	4	−8	1	5	0	0	2
1911.906755	X	cos	+3.54	1	0	0	0	0	−10	3	0	0	0	0	0	0
1783.412180	X	cos	+63.80	0	0	0	0	0	0	4	−8	3	0	0	0	0
10468.417077	X	sin	−1292.02	0	2	−2	2	−2	0	0	0	0	0	0	0	0
1783.412180	X	sin	−18.38	0	0	0	0	0	0	4	−8	3	0	0	0	0
14949.752627	X	sin	−2.23	0	0	0	0	0	0	8	−16	4	5	0	0	−2
1916.001320	X	sin	−4.53	0	0	1	−1	1	0	3	−8	3	0	0	0	0
2024.979608	X	sin	−0.12	0	0	0	0	0	0	4	−8	1	5	0	0	−2
1247.830049	X	sin	−0.12	0	0	0	0	0	5	−6	−4	0	0	0	0	−2
12885.017087	X	sin	+0.12	0	0	0	0	0	0	0	0	0	0	0	0	2
1824.144335	X	sin	+0.12	0	0	0	0	0	0	0	0	2	−6	3	0	−2
1667.979832	X	sin	+0.12	0	0	0	0	0	0	4	−8	3	0	0	0	−1
1916.009383	X	sin	+0.12	0	0	0	0	0	0	4	−8	3	0	0	0	1
1667.985943	X	sin	+3.94	0	0	1	−1	1	0	−5	8	−3	0	0	0	0
11321.399513	X	sin	+4.97	0	0	0	0	0	0	8	−16	4	5	0	0	2
1911.906755	X	sin	+8.71	1	0	0	0	0	−10	3	0	0	0	0	0	0
93294.184305	X	sin	+57.28	0	0	0	0	0	0	8	−16	4	5	0	0	0
10468.417077	Y	cos	−1387.00	0	2	−2	2	−2	0	0	0	0	0	0	0	0
14949.752627	Y	cos	−4.00	0	0	0	0	0	0	8	−16	4	5	0	0	−2
1667.985943	Y	cos	−5.30	0	0	1	−1	1	0	−5	8	−3	0	0	0	0
11321.399513	Y	cos	−5.40	0	0	0	0	0	0	8	−16	4	5	0	0	2
1916.009383	Y	cos	−0.20	0	0	0	0	0	0	4	−8	3	0	0	0	1
1667.979832	Y	cos	+0.20	0	0	0	0	0	0	4	−8	3	0	0	0	−1
1916.001320	Y	cos	+6.10	0	0	1	−1	1	0	3	−8	3	0	0	0	0
1540.710562	Y	sin	+0.20	0	0	0	0	0	0	4	−8	1	5	0	0	2
2024.979608	Y	sin	+0.30	0	0	0	0	0	0	4	−8	1	5	0	0	−2
14949.752627	Y	sin	+4.20	0	0	0	0	0	0	8	−16	4	5	0	0	−2
20936.834154	Y	sin	+167.90	0	1	−1	1	−1	0	0	0	0	0	0	0	0

Appendix E: Model CPN$_b$

Tables E.1−E.4 show the series for concise model CPN$_b$. (When implementing the model in software, the coefficients can be rounded to 10 μas without materially affecting the results.) The model requires a total of 227 coefficients, plus those needed for the fundamental arguments, and achieves worst-case accuracy 0.99 mas between 1995 and 2050. The 1800−2200 errors are shown in Figs. 3 and E.1−E.3.

Table E.1. Part 1 of the series for concise model CPN$_b$: polynomial terms in X, Y and $s + XY/2$.

		t	t^2	t^3	t^4
X	−17251	+2 004 191 898	−429 783	−198 618	
Y	−5530	−25 896	−22 407 275	+1901	+1113
$s + XY/2$	+94	+3809	−123	−72 574	
	μas	μas	μas	μas	μas

Table E.2. Part 2 of the series for concise model CPN$_b$: Poisson terms up to order t^2, and Fourier terms.

	l	l'	F	D	Ω	$L_{\rm Ve}$	$L_{\rm E}$	$L_{\rm Ju}$	$L_{\rm Sa}$	p_A	sin	cos	t sin	t cos	t^2 sin	t^2 cos
X	0	0	0	0	1	0	0	0	0	0	−6 844 318	+1329	−3310	+205 833	+2038	+81
Y	″	″	″	″	″	″	″	″	″	″	+1538	+9 205 236	+153 042	+853	+121	−2301
$s + XY/2$	″	″	″	″	″	″	″	″	″	″	−2641				+744	
X	0	0	2	−2	2	0	0	0	0	0	−523 908	−545	+199	+12 814	+156	
Y	″	″	″	″	″	″	″	″	″	″	−459	+573 033	+11 714	−291		−143
X	0	0	2	0	2	0	0	0	0	0	−90 552	+111		+2188		
Y	″	″	″	″	″	″	″	″	″	″	+137	+97 847	+2025	−51		
X	0	0	0	0	2	0	0	0	0	0	+82 169			−2004		
Y	″	″	″	″	″	″	″	″	″	″		−89 618	−1837			
$s + XY/2$	″	″	″	″	″	″	″	″	″	″	−64					
X	0	1	0	0	0	0	0	0	0	0	+58 707	+470	−180	+164		
Y	″	″	″	″	″	″	″	″	″	″	−192	+7387	−1312			
X	1	0	0	0	0	0	0	0	0	0	+28 288					
Y	″	″	″	″	″	″	″	″	″	″		−675	−633			
X	0	1	2	−2	2	0	0	0	0	0	−20 558		+59	+502		
Y	″	″	″	″	″	″	″	″	″	″		+22 438	+460	−67		
X	0	0	2	0	1	0	0	0	0	0	−15 407			+449		
Y	″	″	″	″	″	″	″	″	″	″		+20 070	+345			
X	1	0	2	0	2	0	0	0	0	0	−11 992			+288		
Y	″	″	″	″	″	″	″	″	″	″		+12 903	+268			
X	0	1	−2	2	−2	0	0	0	0	0	−8585			−215		
Y	″	″	″	″	″	″	″	″	″	″		−9593	+192			
X	0	0	2	−2	1	0	0	0	0	0	+5096			−155		
Y	″	″	″	″	″	″	″	″	″	″		−6918	−114			
X	1	0	0	−2	0	0	0	0	0	0	−6245					
Y	″	″	″	″	″	″	″	″	″	″		−123	+140			
X	1	0	−2	0	−2	0	0	0	0	0	−4911			−119		
Y	″	″	″	″	″	″	″	″	″	″		−5331	+110			
X	1	0	0	0	1	0	0	0	0	0	+2512			−74		
Y	″	″	″	″	″	″	″	″	″	″		−3324	−56			
X	1	0	0	0	−1	0	0	0	0	0	+2308			+70		
Y	″	″	″	″	″	″	″	″	″	″		+3144	−52			
X	1	0	2	0	1	0	0	0	0	0	−2053			+59		
Y	″	″	″	″	″	″	″	″	″	″		+2636				
X	1	0	−2	−2	−2	0	0	0	0	0	+2373			+57		
Y	″	″	″	″	″	″	″	″	″	″		+2555	−53			
X	0	0	0	2	0	0	0	0	0	0	+2521					
Y	″	″	″	″	″	″	″	″	″	″		−122	−56			
X	2	0	−2	0	−1	0	0	0	0	0	−1825			−54		
Y	″	″	″	″	″	″	″	″	″	″		−2424				
											μas		μas		μas	

Table E.3. Part 3 of the series for concise model CPN_b: Fourier terms continued.

	l	l'	F	D	Ω	L_{Ve}	L_E	L_{Ju}	L_{Sa}	p_A	sin	cos
X	2	0	0	−2	0	0	0	0	0	0	+1898	
X	0	0	2	2	2	0	0	0	0	0	−1534	
Y	″	″	″	″	″	″	″	″	″	″		+1645
X	2	0	2	0	2	0	0	0	0	0	−1235	
Y	″	″	″	″	″	″	″	″	″	″		+1324
X	1	0	2	−2	2	0	0	0	0	0	+1137	
Y	″	″	″	″	″	″	″	″	″	″		−1234
X	2	0	0	0	0	0	0	0	0	0	+1163	
Y	″	″	″	″	″	″	″	″	″	″		−61
X	1	0	−2	0	−1	0	0	0	0	0	−813	
Y	″	″	″	″	″	″	″	″	″	″		−1076
X	0	0	2	0	0	0	0	0	0	0	+1030	
Y	″	″	″	″	″	″	″	″	″	″		−56
X	0	0	2	−2	0	0	0	0	0	0	−866	
X	0	1	0	0	1	0	0	0	0	0	−556	
Y	″	″	″	″	″	″	″	″	″	″		+853
X	1	0	0	−2	−1	0	0	0	0	0	−604	
Y	″	″	″	″	″	″	″	″	″	″		−800
X	1	0	0	−2	1	0	0	0	0	0	−512	
Y	″	″	″	″	″	″	″	″	″	″		+696
X	0	2	2	−2	2	0	0	0	0	0	−628	
Y	″	″	″	″	″	″	″	″	″	″		+685
X	0	2	0	0	0	0	0	0	0	0	+665	
X	0	1	0	0	−1	0	0	0	0	0	+507	
Y	″	″	″	″	″	″	″	″	″	″		+644
X	1	0	−2	−2	−1	0	0	0	0	0	+406	
Y	″	″	″	″	″	″	″	″	″	″		+522
X	2	0	−2	0	0	0	0	0	0	0	+439	
X	0	0	2	2	1	0	0	0	0	0	−264	
Y	″	″	″	″	″	″	″	″	″	″		+335
X	0	0	0	2	1	0	0	0	0	0	−251	
Y	″	″	″	″	″	″	″	″	″	″		+327
X	1	0	2	2	2	0	0	0	0	0	−306	
Y	″	″	″	″	″	″	″	″	″	″		+327
X	0	1	2	0	2	0	0	0	0	0	+301	
Y	″	″	″	″	″	″	″	″	″	″		−325
X	0	1	−2	0	−2	0	0	0	0	0	+284	
Y	″	″	″	″	″	″	″	″	″	″		+307
X	1	0	2	−2	1	0	0	0	0	0	+231	
Y	″	″	″	″	″	″	″	″	″	″		−304
X	2	0	0	−2	−1	0	0	0	0	0	+230	
Y	″	″	″	″	″	″	″	″	″	″		+304
X	1	1	0	−2	0	0	0	0	0	0	−292	
X	2	0	2	−2	2	0	0	0	0	0	+256	
Y	″	″	″	″	″	″	″	″	″	″		−277
X	0	0	1	−1	1	0	−1	−2	5	0	−123	+204
Y	″	″	″	″	″	″	″	″	″	″	+274	+165
X	0	1	−2	2	−1	0	0	0	0	0	+189	
Y	″	″	″	″	″	″	″	″	″	″		+272
X	0	0	0	2	−1	0	0	0	0	0	+197	
Y	″	″	″	″	″	″	″	″	″	″		+272
X	2	0	2	0	1	0	0	0	0	0	−213	
Y	″	″	″	″	″	″	″	″	″	″		+269
X	1	0	0	2	0	0	0	0	0	0	+262	
X	2	0	0	−2	1	0	0	0	0	0	+162	
Y	″	″	″	″	″	″	″	″	″	″		−221
X	0	1	2	−2	1	0	0	0	0	0	+142	
Y	″	″	″	″	″	″	″	″	″	″		−191
X	1	−1	0	0	0	0	0	0	0	0	+188	
											μas	

Table E.4. Part 4 of the series for concise model CPN_b: Fourier terms continued.

	l	l'	F	D	Ω	L_{Ve}	L_E	L_{Ju}	L_{Sa}	p_A	sin	cos
X	0	1	0	−2	0	0	0	0	0	0	−173	
X	0	0	0	1	0	0	0	0	0	0	−168	
X	1	0	−2	0	0	0	0	0	0	0	+161	
X	1	0	0	−1	0	0	0	0	0	0	−160	
Y	″	″	″	″	″	″	″	″	″	″		−55
X	1	1	0	0	0	0	0	0	0	0	−135	
X	1	0	2	0	0	0	0	0	0	0	+133	
X	2	0	−2	0	−2	0	0	0	0	0	+122	
Y	″	″	″	″	″	″	″	″	″	″		+131
X	1	−1	0	−1	0	0	0	0	0	0	−130	
X	0	0	0	0	0	0	0	2	−5	−1	+57	+96
Y	″	″	″	″	″	″	″	″	″	″	+129	−77
X	2	0	0	0	−1	0	0	0	0	0	+91	
Y	″	″	″	″	″	″	″	″	″	″		+127
X	1	−1	2	0	2	0	0	0	0	0	−114	
X	3	0	2	0	2	0	0	0	0	0	−115	
Y	1	−1	2	0	2	0	0	0	0	0		+123
Y	3	0	2	0	2	0	0	0	0	0		+123
X	1	1	−2	−2	−2	0	0	0	0	0	+112	
Y	″	″	″	″	″	″	″	″	″	″		+121
X	2	0	0	0	1	0	0	0	0	0	+87	
Y	″	″	″	″	″	″	″	″	″	″		−113
X	0	1	−2	−2	−2	0	0	0	0	0	+105	
Y	″	″	″	″	″	″	″	″	″	″		+113
X	1	0	−2	2	−1	0	0	0	0	0	+79	
Y	″	″	″	″	″	″	″	″	″	″		+107
X	1	1	2	0	2	0	0	0	0	0	+99	
Y	″	″	″	″	″	″	″	″	″	″		−106
X	0	0	0	0	0	3	−5	0	0	−2	+82	
Y	″	″	″	″	″	″	″	″	″	″		+90
Y	1	0	−1	0	−1	0	0	0	0	0	+89	
X	1	0	0	0	2	0	0	0	0	0	−79	
Y	″	″	″	″	″	″	″	″	″	″		+85
X	0	0	2	1	2	0	0	0	0	0	+66	
Y	″	″	″	″	″	″	″	″	″	″		−71
X	1	−1	0	−1	−1	0	0	0	0	0	−52	
Y	″	″	″	″	″	″	″	″	″	″		−70
X	0	2	−2	2	−1	0	0	0	0	0	+51	
Y	″	″	″	″	″	″	″	″	″	″		+67
X	1	0	2	2	1	0	0	0	0	0	−53	
Y	″	″	″	″	″	″	″	″	″	″		+66
X	1	0	−2	−4	−2	0	0	0	0	0	+61	
Y	″	″	″	″	″	″	″	″	″	″		+65
Y	0	0	1	−1	1	−8	12	0	0	0		−64
X	3	0	0	0	0	0	0	0	0	0	+63	
X	1	0	0	0	−2	0	0	0	0	0	−56	
Y	″	″	″	″	″	″	″	″	″	″		−61
X	2	0	−2	−2	−2	0	0	0	0	0	−55	
Y	″	″	″	″	″	″	″	″	″	″		−59
X	0	0	0	0	0	1	−1	0	0	0	+59	
X	1	1	2	−2	2	0	0	0	0	0	+51	
Y	″	″	″	″	″	″	″	″	″	″		−56
X	1	0	0	−4	0	0	0	0	0	0	−53	
Y	2	0	2	−2	1	0	0	0	0	0		−53
Y	2	0	−2	−4	−2	0	0	0	0	0		+52
X	2	0	0	−4	0	0	0	0	0	0	−51	
Y	0	0	0	0	0	0	0	2	0	2		+51
											μas	

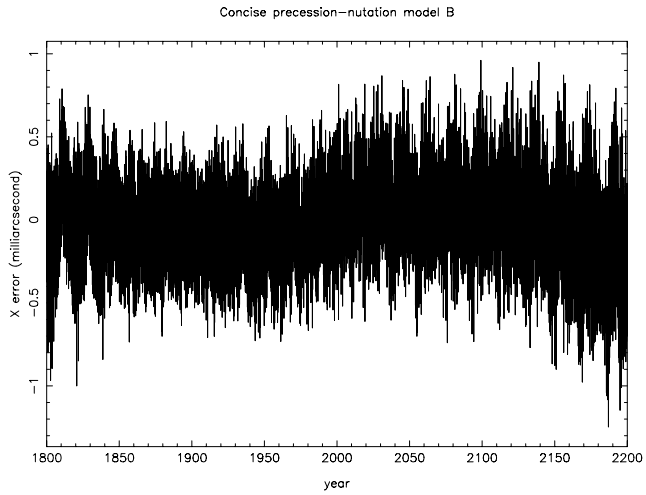

Fig. E.1. CIP X errors in concise formulation CPN$_b$, contributing to the total error shown in Fig. 3.

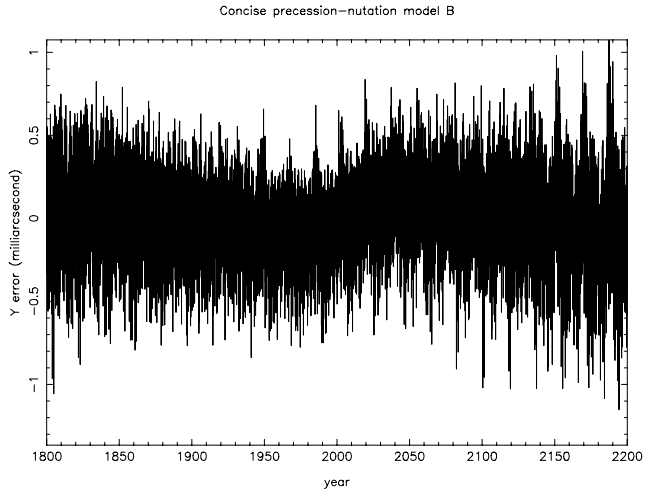

Fig. E.2. CIP Y errors in concise formulation CPN$_b$, contributing to the total error shown in Fig. 3.

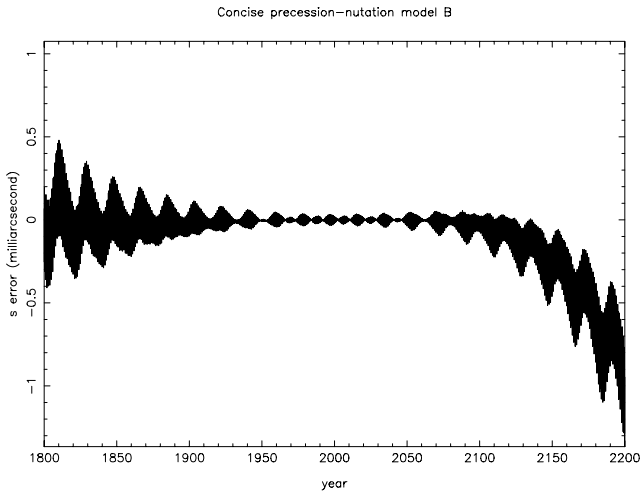

Fig. E.3. CIO errors in concise formulation CPN$_b$, contributing to the total error shown in Fig. 3. CPN$_b$ uses a 7-coefficient $s + XY/2$ series (Sect. 3.2).

Appendix F: Model CPN$_c$

Table F.1 shows the series for concise model CPN$_c$. (When implementing the model in software, the coefficients can be rounded to 100 μas, or even 1 mas, without materially affecting the results.) The CPN$_c$ model requires 45 coefficients, plus a further 10 for the Table C.1 fundamental argument expressions, and achieves worst-case accuracy 16 mas between 1995 and 2050. The 1800−2200 errors are shown in Figs. 4 and F.1−F.3.

Table F.1. The series for concise model CPN$_c$.

Term			Amplitude (μas)	l	l'	F	D	Ω
X			−17 251					
X	t		2 004 191 898					
X	t^2		−429 783					
X	t^3		−198 618					
Y			−5530					
Y	t		−25 896					
Y	t^2		−22 407 275					
$s + XY/2$	t		3809					
$s + XY/2$	t^3		−72 574					
X		sin	−6 844 318	0	0	0	0	1
X	t	sin	−3310	″	″	″	″	″
X	t	cos	+205 833	″	″	″	″	″
Y		cos	+9 205 236	″	″	″	″	″
Y	t	sin	+153 042	″	″	″	″	″
$s + XY/2$		sin	−2641	″	″	″	″	″
X		sin	+82 169	0	0	0	0	2
Y		cos	−89 618	″	″	″	″	″
X		sin	+2521	0	0	0	2	0
X		sin	+5096	0	0	2	−2	1
Y		cos	−6918	″	″	″	″	″
X		sin	−523 908	0	0	2	−2	2
X	t	cos	+12 814	″	″	″	″	″
Y		cos	+573 033	″	″	″	″	″
Y	t	sin	+11 714	″	″	″	″	″
X		sin	−15 407	0	0	2	0	1
Y		cos	+20 070	″	″	″	″	″
X		sin	−90 552	0	0	2	0	2
Y		cos	+97 847	″	″	″	″	″
X		sin	−8585	0	1	−2	2	−2
Y		cos	−9593	″	″	″	″	″
X		sin	+58 707	0	1	0	0	0
Y		cos	+7387	″	″	″	″	″
X		sin	−20 558	0	1	2	−2	2
Y		cos	+22 438	″	″	″	″	″
Y		cos	+2555	1	0	−2	−2	−2
X		sin	−4911	1	0	−2	0	−2
Y		cos	−5331	″	″	″	″	″
X		sin	−6245	1	0	0	−2	0
Y		cos	+3144	1	0	0	0	−1
X		sin	+28 288	1	0	0	0	0
X		sin	+2512	1	0	0	0	1
Y		cos	−3324	″	″	″	″	″
Y		cos	+2636	1	0	2	0	1
X		sin	−11 992	1	0	2	0	2
Y		cos	+12 903	″	″	″	″	″

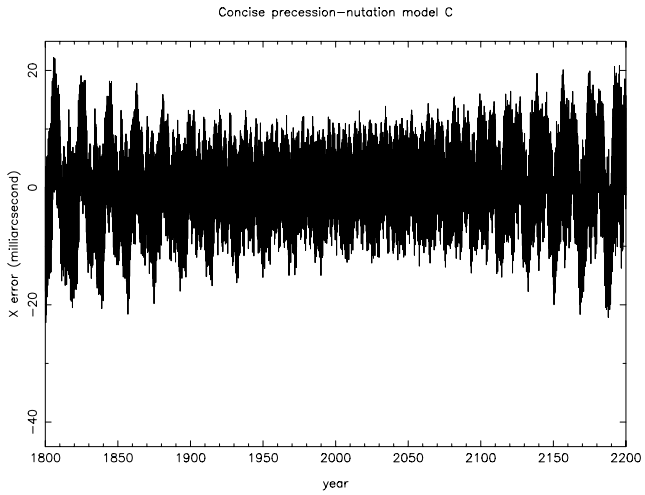

Fig. F.1. CIP X errors in concise formulation CPN$_c$, contributing to the total error shown in Fig. 4.

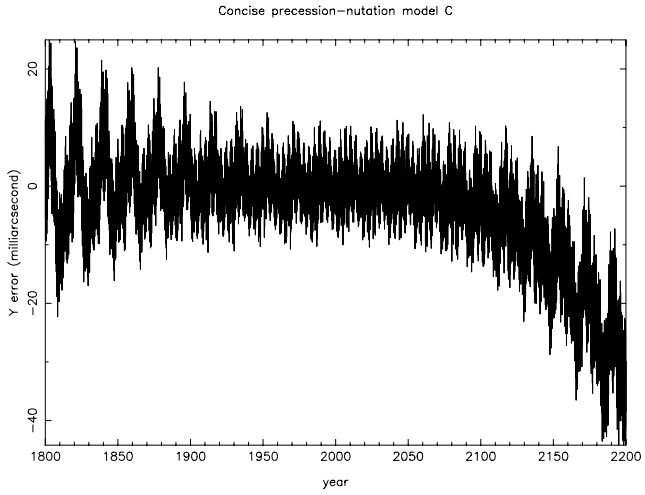

Fig. F.2. CIP Y errors in concise formulation CPN$_c$, contributing to the total error shown in Fig. 4.

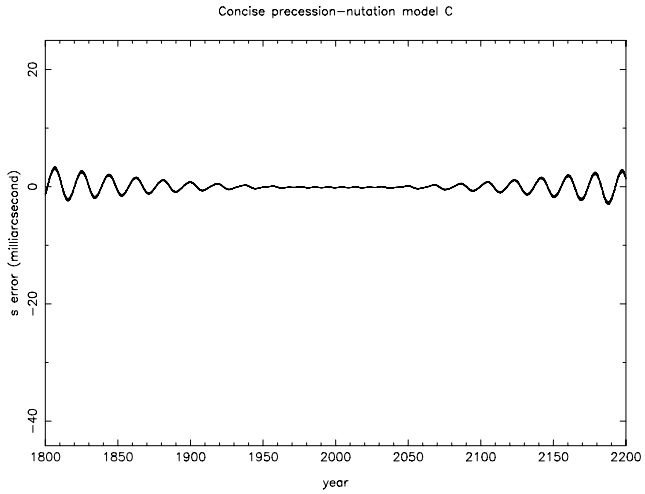

Fig. F.3. CIO errors in concise formulation CPN$_c$, contributing to the total error shown in Fig. 4. CPN$_c$ uses a 3-coefficient $s + XY/2$ series (Sect. 3.2).

Appendix G: Model CPN_d

Table G.1 shows the series for concise model CPN_d. (When implementing the model in software, the coefficients can be rounded to 1 mas, or even 10 mas, without materially affecting the results.) Despite its extreme brevity (only six coefficients), CPN_d achieves worst-case accuracy 0.39 arcsec between 1995 and 2050. The quantity s is neglected, placing the CIO at the line of zero GCRS right ascension, the error contribution from this source being less than 0.1 arcsec throughout the 21st century. The 1800−2200 errors are shown in Figs. 5 and G.1−G.3.

Table G.1. The series for concise model CPN_d.

	Term		Amplitude (μas)	l	l'	F	D	Ω
X	t		2004191898					
Y	t^2		−22407275					
X		sin	−6844318	0	0	0	0	1
Y		cos	+9205236	″	″	″	″	″
X		sin	−523908	0	0	2	−2	2
Y		cos	+573033	″	″	″	″	″

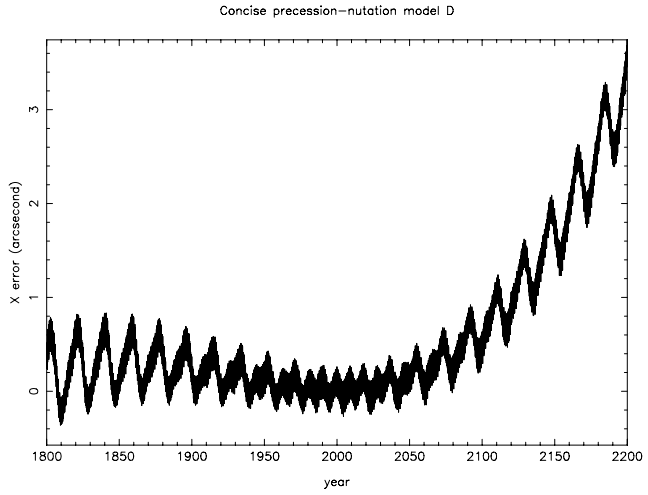

Fig. G.1. CIP X errors in concise formulation CPN_d, contributing to the total error shown in Fig. 5.

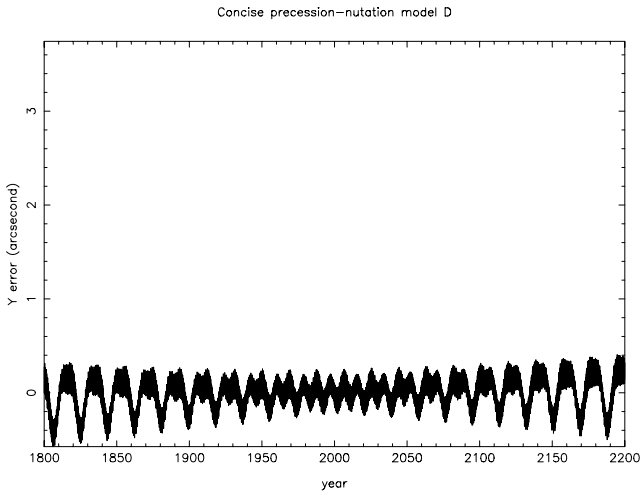

Fig. G.2. CIP Y errors in concise formulation CPN_d, contributing to the total error shown in Fig. 5.

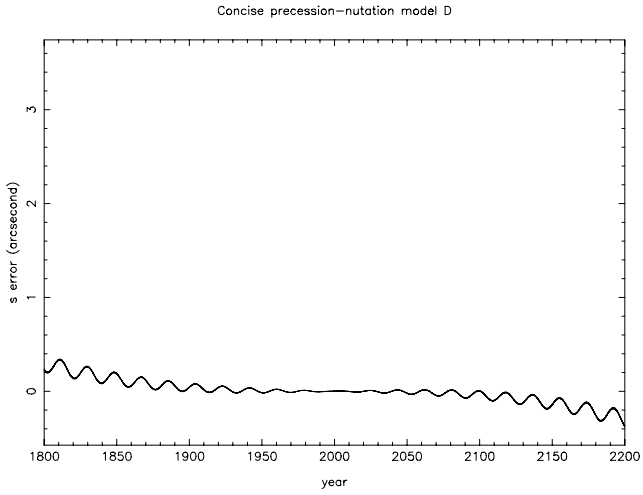

Fig. G.3. CIO errors in concise formulation CPN_d, contributing to the total error shown in Fig. 5. Because CPN_d neglects the quantity s, the plot simply shows $-s$.